



## Radionuclide classification based on gamma spectroscopy and artificial intelligence

Silva<sup>1</sup> M. M. A., Morales<sup>2</sup> R. K., Nunes<sup>3</sup> W. V.,  
Cardoso<sup>4</sup> D. O.

<sup>1,2,3,4</sup>*Instituto Militar de Engenharia / Seção de Engenharia Nuclear (SE/7)*

*Praça General Tibúrcio, 80, 22290-270, Urca, Rio de Janeiro, RJ, Brasil*

<sup>1</sup>*marcio.magalhaes.br@gmail.com, <sup>2</sup>d7karam@ime.eb.br,*

<sup>3</sup>*vallory@ime.eb.br, <sup>4</sup>domin@ime.eb.br*

---

### ABSTRACT

Currently, in almost all segments of the production chain, automation is a requirement for productivity improvement. With respect to nuclear facilities, active online monitoring is one of best practices for nuclear security and safety maintenance, to prevent incidents that could compromise a particular installation. In this context, spectral signature monitoring automation can be explored, aiming at the rapid identification of adverse events, such as radiological accidents. The main objective of this work was an automated radionuclides classification technique establishment, using an Artificial Neural Networks (ANN) architecture. The methodology used consisted basically of simulating the geometry of an established experimental apparatus, using the MCNP5 code, obtaining the simulated gamma spectral signature for the studied nuclides. The simulated spectra were used to compose the ANN training and testing data set, while the experimental spectra were subjected to the artificial intelligence model classification, in order to allow the neural network quality assessment. The final developed architecture of ANN was correct to recognize the experimental spectra of <sup>60</sup>Co, <sup>137</sup>Cs and <sup>152</sup>Eu. Therefore, the results were satisfactory and proved automation technique development viable.

*Keywords: Gamma Spectroscopy, Artificial Intelligence, Artificial Neural Networks.*

---



## 1. INTRODUCTION

Currently, there are constant changes in labor relations and in the productivity increase in the industry and services sectors, based on artificial intelligence solutions. Regarding the nuclear installations area, there are points that deserve attention, especially those dealing with these installations safety, as critical events such as leaks, radioactive elements dispersion in the atmosphere and even nuclear material theft may, not only compromise physical safety of a plant, but also exposing the public to hazardous conditions. In this context, artificial intelligence, especially supervised machine learning, can offer an agile way of detecting security incidents, allowing for quick action by the team responsible for the installation.

The main purpose of this work is to establish an automated classification model for radionuclides based on Artificial Neural Networks (ANN). The basic study concept is to simulate the gamma spectral signature of the nuclides studied set, through the MCNP5 code, to compose the ANN training and tests set. Then, the model is validated with data obtained from the experimental survey of the spectra of some of these nuclides.

Studies with models similar to the one proposed, using computational simulation based on the Monte Carlo method for ANN training, which aim at spectra classification, appear in the literature already in the nineties, as in the work of FUKUDA and KITAMURA [1]. In this study, the real-time analysis of spectra was sought for nuclear safety purposes. In fact, a functional model was arrived at, but it was concluded that there was still a need for additional studies due to the incipience of the technique at the time.

In 2005, the work of NUNES [2] used the ANN training model based on simulation with the use of the MCNP, for detection of landmines, based on the recognition of characteristic gamma spectra patterns, resulting from the activation of the materials present in the explosives by thermal neutrons. The result obtained shows that not only the ANN was able to recognize the patterns of the soil compositions where it was trained, but also acted in the identification of the presence of mines in situations outside this scope.

In 2015, the work of VARLEY [3] used an ANN application, with training based on simulation data with the MCNP, in order to identify traces of  $^{226}\text{Ra}$ , resulting from military activities in the

United Kingdom. It is concluded that the technique provided a reliable means for estimating the activity of point sources and information on possible layers of soil contamination.

Recently, in 2020, JHUNG et al. [4] used an ANN to identify gamma-emitting radionuclides using silicon photomultipliers. In this case, the training was carried out with experimental spectra, different from the spectra submitted to classification. It was concluded that the network was able to classify them correctly, and that increasing the depth of the network can improve the classification results.

In this context, and in addition to the main proposal, the study led to the possibility of enabling a model that could support an alternative project to the use of detectors available on the market, which despite offering the functionality of spectra classification, are proprietary technology. Thus, the artificial intelligence model used in this work will be able to establish the pillars of a software that can compose the core of an industrial automation system, which, in turn, aims at the automated monitoring of the spectral signature of a nuclear installation.

## 2. MATERIALS AND METHODS

In order to facilitate the understanding of the various steps of the experiments carried out, this study was divided into two phases. The first phase consisted of defining the experimental apparatus, reproducing this apparatus in the computational environment of the MCNP5[5] code, comparing the simulated and experimental spectra of  $^{137}\text{Cs}$ ,  $^{60}\text{Co}$  and  $^{152}\text{Eu}$ , and validating the initial configuration of the ANN. The second phase consisted of expanding the nuclides present amount in the training and testing base, and adjusting the ANN parameterization, so that it produces results consistent with this new knowledge base.

The Neural Network implementation was made using the Python programming language [6], Keras [7] and Tensorflow [8] frameworks, used within Google's collaborative computing environment, Colab[9]. The main metric for monitoring the performance of the ANN versions used in the experiments performed was the loss function, using the cross entropy algorithm [10], with the accuracy function as a secondary metric.

## 2.1. First phase

The equipment used to assemble the experimental apparatus consisted of: (i) A sealed source of  $^{60}\text{Co}$ , with an activity of 7.49 kBq; (ii) A sealed source of  $^{137}\text{Cs}$ , with an activity of 27.76 kBq; (iii) A sealed source of  $^{152}\text{Eu}$ , with activity of 81.84 kBq (the activity of the sources on the day of the experiment is considered, with an associated error of 5%); (iv) a set formed by a scintillator type detector, NaI(Tl) and a Canberra model 802-3”X3” photomultiplier valve; (v) Ortec pre-amplifier, model 113; (vi) BIN Ortec, model 4001C; (vii) Ortec high voltage source, model 556; (viii) Canberra amplifier, model 2022; (ix) MCB Ortec module, model 926; (x) MCB cable, model DPM-USB; (xi) Computer; (xii) ORTEC Maestro 32 R Software, version 7.01; (xiii) Amprobe multimeter model HD110C and (xiv) Tektronix oscilloscope model TBS1064.

The experimental apparatus schematic geometry can be seen in figure 1.a. The colors present in the illustration are representative of the materials used, broken down in figure 1.b, and detailed in table 1. Some proportions, especially the parts of the detector with thicknesses less than 2 mm, were suppressed in the figure to improve the scheme visualization. Material 4, shown in figure 1, is decomposed into other 3 materials in table 1, representing the composition of a 1 mm thick Neoprene disc (material 4.b) and a polyethylene disc (material 4.c) of 0.15 mm, plus a 0.5 mm layer representing the detector Aluminum case (Material 4.a). The construction details of the detector were based on the detector schematic diagram (MIRION [11]) and on the work of MEDEIROS [12]. The uncertainty associated with geometric measurements is 0.1 mm.

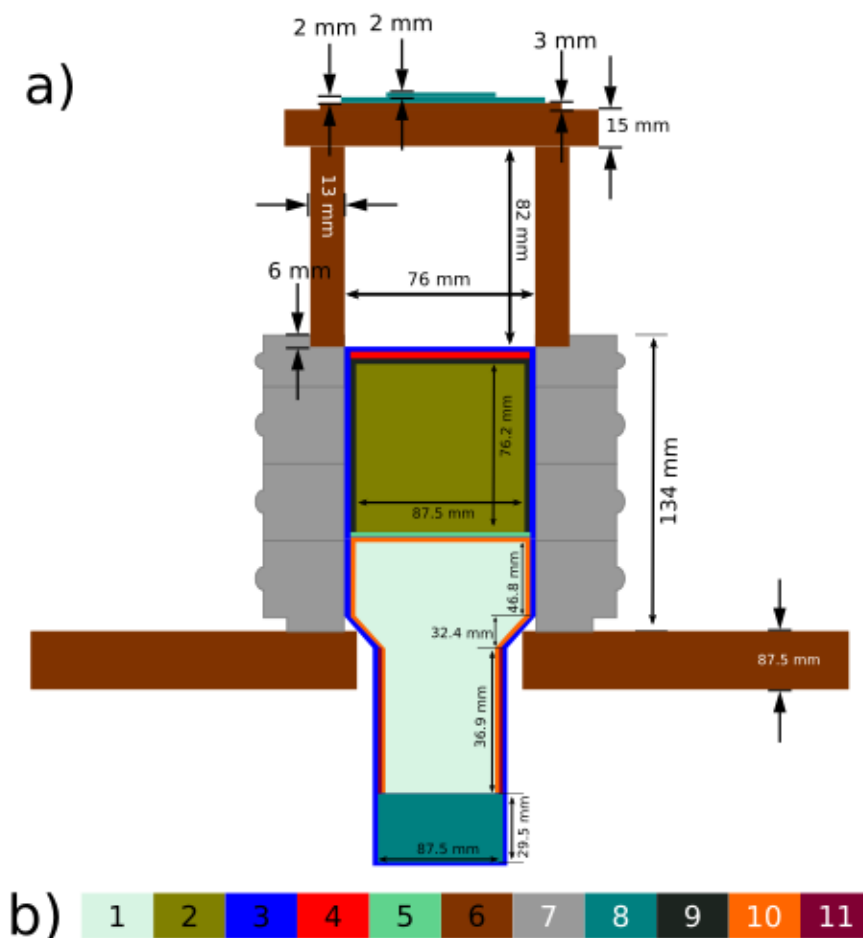


**Figure 1:** a) Schematic view of the apparatus geometry; b) Representation of the materials used in the apparatus, detailed in table 1.

The experimental spectra obtained were used in the calibration of the detection system, with the variability of the uncertainty associated with the count statistics being within acceptable limits (given by  $n^{1/2} / n$ , where  $n$  is the counts number of a given spectrum, in the region that forms the Gaussian of each of its photopeaks). After the experimental survey of the  $^{137}\text{Cs}$ ,  $^{60}\text{Co}$  and  $^{152}\text{Eu}$  spectra, the experimental apparatus was reproduced within the computational environment of MCNP5.

The simulation was performed on a computer with an Intel(R) Core(TM) i7-8700 3.2 GHz processor (6 physical cores and 12 logical cores), with 8 Gb RAM memory installed, running

Windows 10 Home operating system 64-bit. In the simulations, 385 million stories were used for each nuclide, with an average simulation time of 10 hours, using 10 cores.

**Table 1:** Materials used in the apparatus and reproduced in the simulation (numbering illustrated in figure 1). The numbers in parentheses in the second column represent the percentage by mass of each element.

<b>Material Details</b>		
<b>Mat.</b>	<b>Chemical Composition/Mass Proportion (%)</b>	<b>Density (g / cm<sup>3</sup>)</b>
<b>1</b>	Vaccum	-
<b>2</b>	Na (15,34) / I (84,66)	3,66
<b>3</b>	Al (100)	2,69
<b>4.a</b>	Al (100)	2,69
<b>4.b</b>	H (8) / O (52) / Cl (40)	1,23
<b>4.c</b>	H (14,37) / C (85,63)	0,93
<b>5</b>	H (8,1) / C (32,1) / O (22,3) / Si (37,5)	1,0185
<b>6</b>	H (5,96) / C (49,7) / N (0,5) / O (2,74) / Mg (0,2) / S (0,5) / K (0,2) / Ca (0,2)	0,64
<b>7</b>	Pb (100)	11,35
<b>8</b>	H (8,05) / C (59,99) / O (31,96)	1,19
<b>9</b>	O (39,7) / Mg (60,3)	0,55
<b>10</b>	O (15,64) / Si (8,1) / Ti (0,8) / As (0,26) / Pb (75,19)	6,22
<b>11</b>	C (0,17) / Fe (99) / Mn (0,75) / P (0,35) / S (0,45)	1,1805

The source was modeled in the MCNP as a fixed planar source, from a 110 mm distance of detector outermost wall. The data on gamma emission energies and their respective intensities for the radionuclides used were based on information contained in LARAWEB [13]. The simulations considered photons and electrons as types of particles existing in the model, and used the ENDF/B-VI library as a cross section table. All simulations obtained a value less than 0.1 in the verification of counting fluctuation (Tally Fluctuation Chart) of the MCNP5 output files.

From the simulation model, the simulated spectra of the aforementioned nuclides were obtained, using the Tally F8 and the GEB function (Gaussian Energy Broadening, a function that simulates the energy resolution of a real radiation detector [5], using the parameters a, b and c with the estimated values at  $-9.3408 \times 10^{-3}$ ,  $7.5107 \times 10^{-2}$  and 0.5843 respectively). Once the experimental and simulated spectra were obtained, a visual analytical comparison was performed, which consisted of the graphic overlay between these spectra.

After the graphic analysis described, the spectra obtained from the simulation model were used as a dataset for testing and training the ANN. The experimental apparatus and the geometry visualization within the Vised Software are illustrated in figure 2.a and 2.b, respectively.

The starting point of the ANN used in this first phase was based on the architecture of the study by NUNES [2], with some necessary adjustments to adapt to the data sets used. The initial configuration consisted of a 3-layer network, with the first layer containing 128 neurons, using the hyperbolic activation function, the second layer containing 64 neurons, using the Gaussian complementary activation function, and the third layer containing 3 neurons, using the function of softmax activation. The model used a learning rate of 0.1 and 3600 epochs of training. Initialization of weights is done randomly by default by Keras. The production data set used were the spectra obtained experimentally from the  $^{137}\text{Cs}$ ,  $^{60}\text{Co}$  and  $^{152}\text{Eu}$  nuclides.

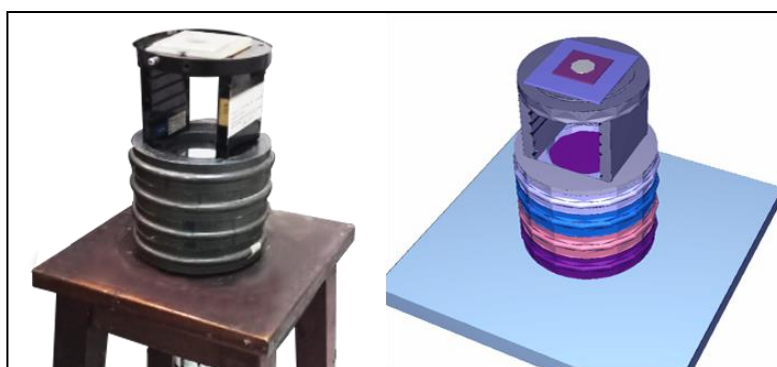


**Figure 2:** a) *Experimental apparatus;* b) *Reproduction of the apparatus with Vised software*

## 2.2. Second phase

In this phase, the nuclide types (classes for ANN) of the ANN training and tests sets were expanded, in order to include a total of 24 distinct radionuclides ( $^{140}\text{Ba}$ ,  $^{131}\text{I}$ ,  $^{135}\text{I}$ ,  $^{85\text{m}}\text{Kr}$ ,  $^{132}\text{Te}$ ,  $^{133}\text{Xe}$ ,  $^{133\text{m}}\text{Xe}$ ,  $^{135}\text{Xe}$ ,  $^{137}\text{Cs}$ ,  $^{60}\text{Co}$ ,  $^{241}\text{Am}$ ,  $^{226}\text{Ra}$ ,  $^{192}\text{Ir}$ ,  $^{238}\text{Pu}$ ,  $^{210}\text{Po}$ ,  $^{252}\text{Cf}$ ,  $^{238}\text{U}$ ,  $^{235}\text{U}$ ,  $^{40}\text{K}$ ,  $^{232}\text{Th}$ ,  $^{152}\text{Eu}$ ,  $^{133}\text{Ba}$ ,  $^{57}\text{Co}$ ,  $^{54}\text{Mn}$ ), whose spectra were obtained from simulation with the MCNP5. This inventory was selected based on the studies by CURZIO[14], who developed a radioactive plume dispersion analysis resulting from a simulated accident with a small PWR reactor and PEREIRA[15], which analyzes a hypothetical dirty bomb explosion at a large public event. The radionuclides stored in the laboratory of the Instituto Militar de Engenharia (IME) were kept in the inventory, namely  $^{152}\text{Eu}$ ,  $^{133}\text{Ba}$ ,  $^{57}\text{Co}$ ,  $^{60}\text{Co}$  and  $^{54}\text{Mn}$ , in addition to  $^{137}\text{Cs}$ , present in the inventory surveyed by CURZIO[14]. The experimentally obtained spectra of  $^{137}\text{Cs}$ ,  $^{60}\text{Co}$  and  $^{152}\text{Eu}$  were again used as ANN production data.

In this phase, the ANN configuration was started with the same final configuration of the first phase, which, when submitted to a new set of training data and tests, did not obtain satisfactory performance. A systematic evolution was carried out with alteration of several ANN parameters, having as indicators of improvement the curves of the loss and accuracy functions, as mentioned above. The final configuration obtained in this phase was an ANN with four layers, obtained by inserting a hidden layer before the output layer of the previous configuration, with 32 neurons and using the sigmoid activation function. In addition, hyper parameters such as learning rate, learning batch size [16], and the optimization algorithm were changed, the latter causing a significant improvement in the results, using ADAM[17] from this phase on.



### 3. RESULTS AND DISCUSSION

The work had as its starting point the ANN architecture of the study by NUNES [2], differing in the application of the classifier, obtaining assertiveness similar to the work cited. Thus, a neural network capable of distinguishing between the spectra submitted to classification within the set of radionuclide spectra that composed the training base of the network was obtained.

The comparison with the studies of VARLEY [3] and JHUNG et al.[4] shows that, like the aforementioned authors, this study shows the feasibility of using Artificial Neural Networks for the classifiers implementation within the nuclear area.

Next, the results obtained will be described, as well as the relevant discussions, referring to each experiment phase in the respective subsequent sections.

#### 3.1. First phase

Once the experimental apparatus was defined and assembled, the energy calibration of the detection system was performed [18,19] with the nuclides  $^{60}\text{Co}$ ,  $^{152}\text{Eu}$  and  $^{137}\text{Cs}$ . Figure 3 shows the visual comparison between the graphically superimposed experimental and simulated spectra for the defined experimental apparatus.

A visual adhesion, illustrated in Figure 3, was observed between the experimental and simulated spectra for 3 used nuclides. However, there are some deviations between the overlapping spectra, which may require a detailed analysis in a future study.

Once the simulation results were validated with the data obtained experimentally, the Neural Network used as the main point of the automated radionuclide classification system was parameterized. Thus, after using the analytical comparison to validate the computational simulation model, the simulation data, as well as the experimental spectra, were submitted to classification with the ANN configured in the first phase of the experiment. The loss and accuracy curves obtained from this classification are illustrated in Figure 4. The classification result is shown in table 2.

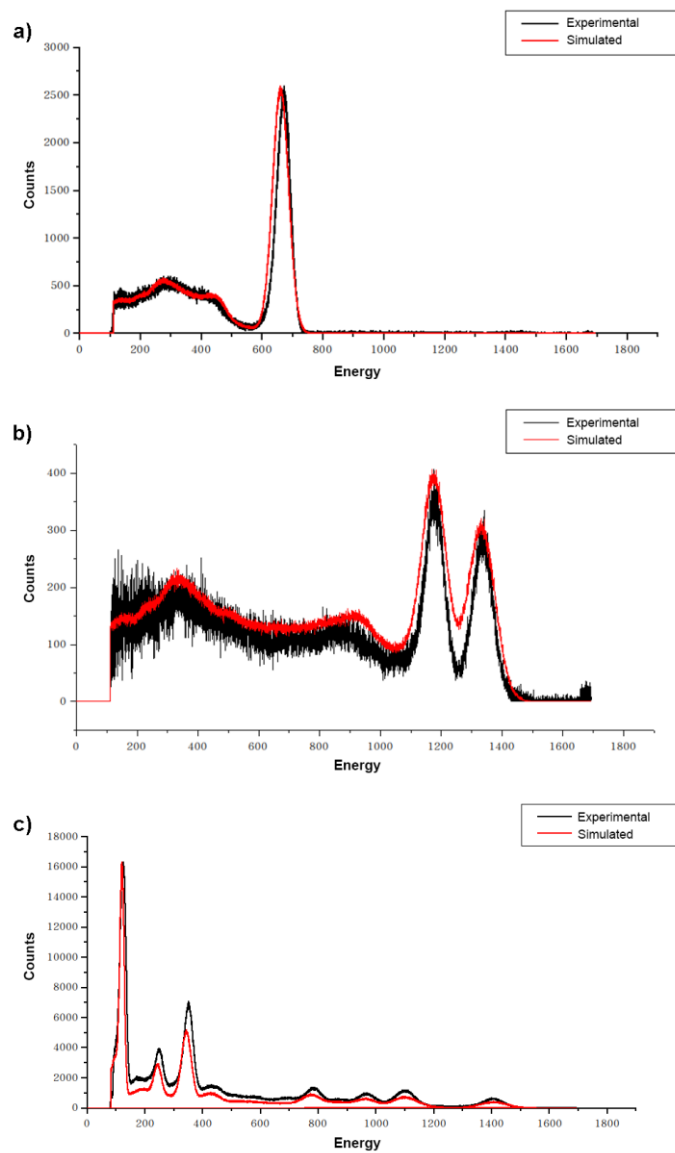


**Figure 3:** Comparison between experimental and simulated spectra for (a)  $^{137}\text{Cs}$ , (b)  $^{60}\text{Co}$  e (c)  $^{152}\text{Eu}$ .

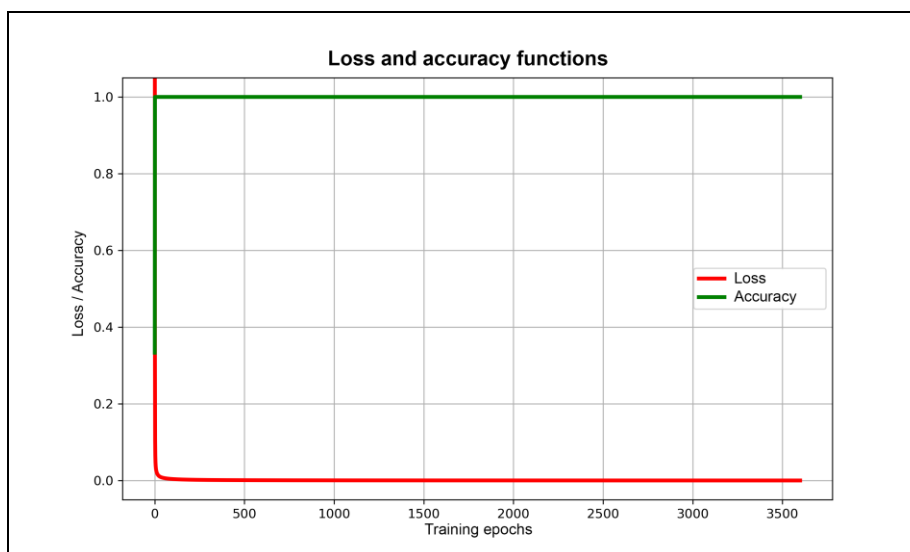


**Figure 4:** Loss and accuracy function curves obtained in the first phase of the experiment.

**Table 2:** Classification result obtained in the first phase.

Source	Pertinence Relations		
	$^{60}\text{Co}$	$^{137}\text{Cs}$	$^{152}\text{Eu}$
$^{60}\text{Co}$	9,96e-01	2,71e-03	7,83e-04
$^{137}\text{Cs}$	6,58e-04	9,98e-01	6,71e-04
$^{152}\text{Eu}$	7,47e-03	8,83e-03	9,83e-01

### 3.2. Second phase

The results obtained in the second phase of the experiment, with the four-layer ANN configured as described in section 2.2, relating to the curves of the loss and accuracy functions are illustrated in Figure 5. The result of the separation into classes for each nuclide is shown in the table 3. The pertinence relations with the other nuclides in the knowledge base were omitted as they were negligible.

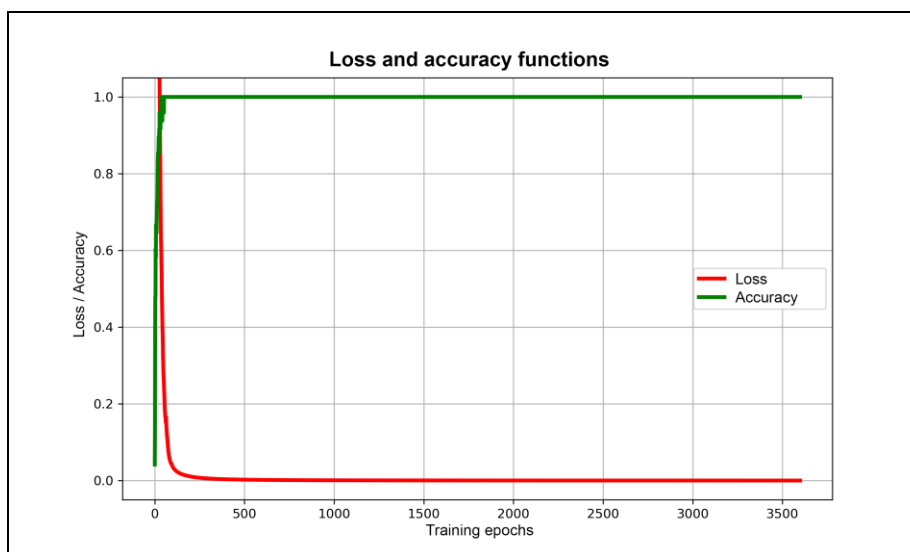


**Figure 5:** Loss and accuracy function curves obtained in the second phase of the experiment.

**Table 3:** Classification result obtained in the second phase.

Source	Pertinence Relations		
	$^{60}\text{Co}$	$^{137}\text{Cs}$	$^{152}\text{Eu}$
$^{60}\text{Co}$	9,99e-01	3,23e-08	2,25e-06
$^{137}\text{Cs}$	3,70e-08	9,99e-01	2,66e-06
$^{152}\text{Eu}$	5,01e-04	4,58e-05	9,90e-01

It was possible to observe that the curves of the loss and accuracy functions quickly tended to zero and one respectively, over the training epochs, with the final loss being  $1.5170 \times 10^{-4}$  in the first phase and  $2.335 \times 10^{-5}$  with respect to the second phase. In addition, all pertinence relations, obtained through the classification of nuclides used as production data, returned results above 0.98, which would perfectly suit a practical application of the study.

## 4. CONCLUSION

The study carried out had as its main proposal to establish an automated classification model for radionuclides, based on the Artificial Neural Networks application and supervised machine learning. In fact, it was described how the application of ANN can produce viable results for the development of an automation technique, in order to meet this project requirement.

Furthermore, having a path that can be developed in order to obtain a viable alternative to detectors with similar functionality, high cost and available only from international manufacturers, contributes to the strengthening of national industry and technology with regard to the applications of radiological defense.

It should also be noted that the implementation of the ANNs in this study was carried out with free and open source technologies, such as the Python language, and the Keras and TensorFlow libraries, which brings the versatility needed to make the developed models part of a customized automation system .

A continuation of this study may aim at an automation system with a core based on artificial intelligence, which can be configured, for example, to monitor the spectral signature of a specific type of nuclear installation, aiming at increasing its radiological safety.

Another future study, derived from this work, would be the use of Deep Learning, as suggested in the study by JHUNG et al. [4], with the substantial increase of layers in the used neural network, which could serve as a work proposal whose objective would be to compare the results to be obtained with the results of the present study.

## REFERENCES

- [1] FUKUDA, H.; KITAMURA, S. I. **Application of Projection Neural Network to Monitoring for Environmental Gamma Radiation**. In: Radiation Detectors and Their Uses, 8., 1994, Tsukuba. Anais[...]. Tsukuba: National Laboratory for High Energy Physics (KEK). Available at: <[https://inis.iaea.org/collection/NCLCollectionStore/\\_Public/26/074/26074201.pdf](https://inis.iaea.org/collection/NCLCollectionStore/_Public/26/074/26074201.pdf)>. Last accessed: 08 Apr. 2021.

- [2] NUNES, W. V. **Detecção de minas terrestres por radiação penetrante**. Universidade Federal do Rio de Janeiro, 2005. 123p.
- [3] VARLEY, A. et al. **Development of a neural network approach to characterise  $^{226}\text{Ra}$  contamination at legacy sites using gamma-ray spectra taken from boreholes**. *Journal of environmental radioactivity*, v. 140, p. 130–140, 2015. Available at: <<https://doi.org/10.1016/j.jenvrad.2014.11.011>>. Last accessed: 08 Apr. 2021.
- [4] JHUNG, S.; HUR, S.; CHO, G.; KNOW, I. **A neural network approach for identification of gamma-ray spectrum obtained from silicon photomultipliers**. *Nuclear Instruments and Methods in Physics Research Section*, v. 954, 2020. DOI 10.1016/j.nima.2018.12.019. Available at: <<https://doi.org/10.1016/j.nima.2018.12.019>>. Last accessed: 08 Apr. 2021.
- [5] X-5 Monte Carlo Team, **MCNP - Version 5, Vol. I: Overview and Theory**, LA-UR-03-1987 (2003).
- [6] ROSSUM, G. V., et al. **Python Reference Manual**. Python Software Foundation. 2020. Available at: <<https://docs.python.org/3/download.html>>. Last accessed: 31 Oct. 2020.
- [7] CHOLLET, F., et al. **Keras**. 2015. Available at: <<https://github.com/fchollet/keras>>. Last accessed: 31 Oct. 2020.
- [8] ABADI, M., et al. **TensorFlow: Large-scale machine learning on heterogeneous systems**. 2015. Available at: <<https://www.tensorflow.org>>. Last accessed: 31 Oct. 2020.
- [9] GOOGLE LLC. Colaboratory. Available at: <<https://colab.research.google.com>>. Last accessed: 31 Oct. 2020.
- [10] DAS R., CHAUDHURI S. **On the Separability of Classes with the Cross-Entropy Loss Function**. arXiv e-prints (Cornell University), 2019. Available at: <<https://arxiv.org/pdf/1909.06930.pdf>>. Last accessed: 02 Nov. 2020.
- [11] MIRION TECHNOLOGIES. 802 Scintillation Detectors. Available at: <[https://mirion.s3.amazonaws.com/cms4\\_mirion/files/pdf/specsheets/csp0232\\_802\\_super\\_spec\\_2.pdf](https://mirion.s3.amazonaws.com/cms4_mirion/files/pdf/specsheets/csp0232_802_super_spec_2.pdf)>. Last accessed: 08 Apr. 2021.
- [12] MEDEIROS, M. P. C et al. **Gamma absorption coefficients calculation by Nai(Tl) detector and computer modelling in MCNPX code**. In: International Nuclear Atlantic Conference, 2015, São Paulo. Anais[...]. Rio de Janeiro: Associação Brasileira De Energia Nuclear - Aben, 2015.

- [13] LARAWEB, Library for gamma and alpha emissions. Laboratoire National Henri Becquerel. Available at: <<http://www.nucleide.org/Laraweb/index.php>>. Last accessed: 08 Apr. 2021.
- [14] CURZIO, R. C., et al. **Modelagem computacional da dispersão atmosférica aplicada a um reator modular de pequeno porte**. Brazilian Journal of Radiation Sciences. 2020
- [15] PEREIRA, J.F. **Explosão de bomba suja em local de grande evento público: uma metodologia para ações de emergência**. CNEN/IRD, 2018. 124p.
- [16] HAYKIN, S. **Neural Networks and Learning Machines**, 3<sup>rd</sup> ed. New Jersey: Pearson Education Inc., 2009.
- [17] KINGMA, D. P., BA, J. L. Adam: A Method for Stochastic Optimization. In: **International Conference on Learning Representations**, 2015, San Diego. Annals... San Diego, 2015. Available at: <<https://arxiv.org/pdf/1412.6980.pdf>>. Last accessed: 02 Nov. 2020.
- [18] TSOULFANIDIS, N., LANDSBERGER, S. **Measurement & Detection of Radiation**, 4<sup>rd</sup> ed. Boca Raton: Taylor & Francis Group, 2015.
- [19] KNOLL, G. F. **Radiation Detection and Measurements**, 4<sup>rd</sup> ed. New York: John Wiley & Sons Inc, 2010.